Analytical Platform to Characterize Dopant Solution Concentrations, Charge Carrier Densities in Films and Interfaces, and Physical Diffusion in Polymers Utilizing Remote Field-Effect Transistors

Hyun-June Jang, Justine Wagner, Hui Li, Qingyang Zhang, Tushita Mukhopadhyaya, Howard E. Katz*

Department of Materials Science and Engineering, Johns Hopkins University, 3400 N. Charles St, Baltimore, USA

Experimental Section

1. Sample preparations

ITO/PET (Sigma Aldrich, 639303) and ITO/glass (Sigma Aldrich, 50926-11-9) substrates were purchased and processed as below. The substrates were sliced into 1 cm × 2 cm dimensions for the remote electrode. Before using, the substrates were cleaned with isopropanol for 20 min under ultrasonication, then rinsed with distilled water for 20 min, and dried under nitrogen gas. SiO_2/Si substrates, with a 70 nm and 300 nm thickness of oxide, were also prepared via standard RCA cleaning process. A concentration of 10 mg/ml of poly-3-hexylthiophene (P3HT) (Solaris, SOL4106) was prepared by dissolving polymer in chlorobenzene, sonicating for 1 hour, and then heating at 60 °C overnight, respectively. Polystyrene (PS) (Sigma Aldrich, 430102) solutions were prepared at concentrations of both 10 mg/ml and 35 mg/ml PS and were dissolved in toluene under ultrasonication. In order to synthesize polystyrene-co-4-vinylbenzocyclobutane (XLPS), a solution of styrene, 4-vinylbenzocyclobutane (10% in weight ratio), and 2,2′- azobis(isobutyronitrile) (AIBN, 2% in weight ratio) in chlorobenzene (2 mL for 10 mmol total monomers) in a high-pressure vessel was bubbled with nitrogen for 10 min and then sealed rapidly under a nitrogen atmosphere. The mixture was stirred vigorously at 65 °C for 18 h in the dark. After cooling to room temperature, the resulting viscous solution was precipitated into methanol (150 mL) and stirred for 1 h. The precipitated polymer was dissolved in tetrahydrofuran (THF) and then reprecipitated into methanol. The purification procedure was repeated twice, and the precipitate was dried under vacuum (at 60 °C in the vacuum oven) to yield XLPS in 90% yield. The concentrated solutions were then filtered using a hydrophobic PTFE syringe filter. The solutions were then applied to the substrates indicated above by spin coating. P3HT, PS, and XLPS were spin coated on SiO_2/Si, ITO/PET, and ITO/glass substrates

under 1800 RPM for 1 min, respectively. Post annealing of P3HT and PS was done using heat plate under 60 °C and 100 °C for 1 h. XLPS was baked in vacuum oven for cross-linking under 180 °C for 2 h. The surface images of each P3HT were acquired by using the Optical Profilometer/3D laser scanning microscope (VK-X100). The P3HT and PS film had a thickness of 46.5 nm and 200 nm measured using the Thin Film Analyzer (F20-NIR). A 1 mg/mL solution of F4TCNQ (Ossila, 29261-33-4), TCNQ (Alfa Aesar, 1518-16-7), and TCNE (Sigma Aldrich, 670-54-2) was prepared by dissolving the dopant in acetonitrile aided by ultrasonication for 30 minutes, filtered using a hydrophobic PTFE syringe filter membrane, and then a series dilution was conducted in order to create the range of solution concentrations from 1 mg/ml to 100 ng/ml.

2. UV-Vis-NIR spectroscopy and XPS

Doping was performed by wetting the surface of pure P3HT film on ITO with each F4TCNQ solutions in different concentrations, waiting 5 seconds, then spinning off the excess solution at 1800 rpm. **A**bsorption peak intensity was measured with a LAMBDA 950 UV/Vis Spectrophotometer with incremental increase of wavelength by 1 nm. All spectra were normalized to 1 at the maximum of the P3HT absorption at 540 nm. The X-ray Photoelectron Spectroscopy (XPS) spectra were analyzed using a PHI 5600 XPS (58.7 eV pass energy, 0.250 eV/step, Mg Kα X-rays) and processed with CasaXPS software (Teignmouth, UK).

3. Conductivity and capacitance samples

Sheet resistance of each doped P3HT film on SiO_2/Si processed identically above was measured by four-point probes measurements. To make contact on the four-point probe, Au was deposited on doped P3HT film with a shadow mask (width: 2 mm and length: 250 μm between two Au electrodes). In order to measure the capacitance of P3HT/SiO_2, the area of doped P3HT

for the capacitor was defined by O_2 plasma etching using Au gate mask with 4 types of length: 0.95, 1.1, 1.25, and 1.4 mm and the same width of 2 mm.

4. Field-effect transistor (FET) detection system

The FET detection system was divided into two parts: a FET (CD4007UB) and a RG module. Si used as electrode for P3HT/SiO_2/Si substrate on a RG module was electrically coupled to the gate of FET. 25 μl of each varying concentration of dopant dissolved in acetonitrile was placed on the P3HT surface of the RG module and a Ag/AgCl reference electrode was placed in the solution in order to apply the gate bias for all measurements. Any potential variation on the RG modules would be transferred to the gate of the FET by shifting the threshold voltage (V_{th}). All transfer curves were measured by using a Keithley semiconductor analyzer with a drain voltage set at 50 mV and the gate voltage left at double sweep mode. The V_{th} was extracted from the gate voltage which corresponded to a drain current of 1 μA. After the stabilization process, varying concentration solutions of F4TCNQ, from low to high concentrations, were placed on the surface of each RG module and V_{th} shifts were monitored. After injecting 1 mg/ml of F4TCNQ solution, remote modules were then repeatedly washed 3 times with pure acetonitrile (ACN) and then the remote-gate (RG) was remeasured under a new pure ACN. pH sensitivity of ITO RG was evaluated by using standard pH buffer solution.

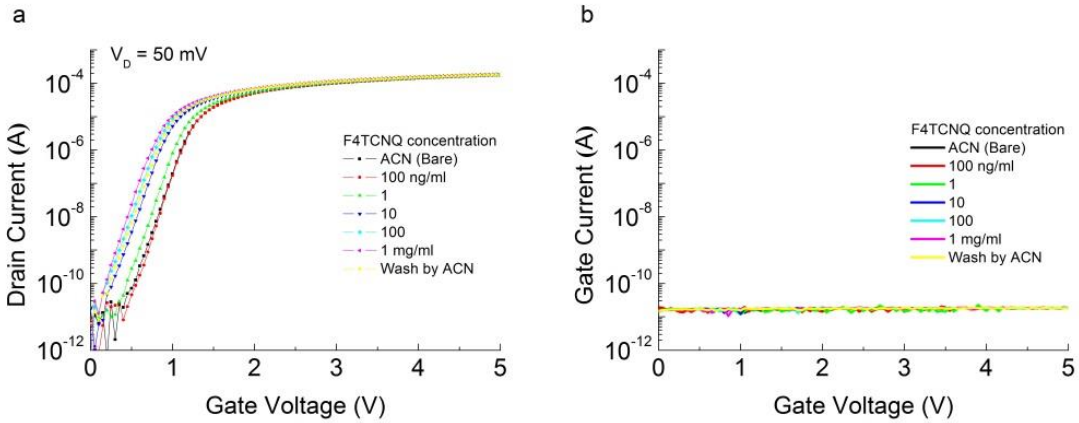

Figure S1. (a) Representative response of transfer curves of remote-gate field effect transistor (RG FET) to F4TCNQ solution concentration with a P3HT RG. (b) Gate leakage currents measured in the transfer curves in Figure S1a.

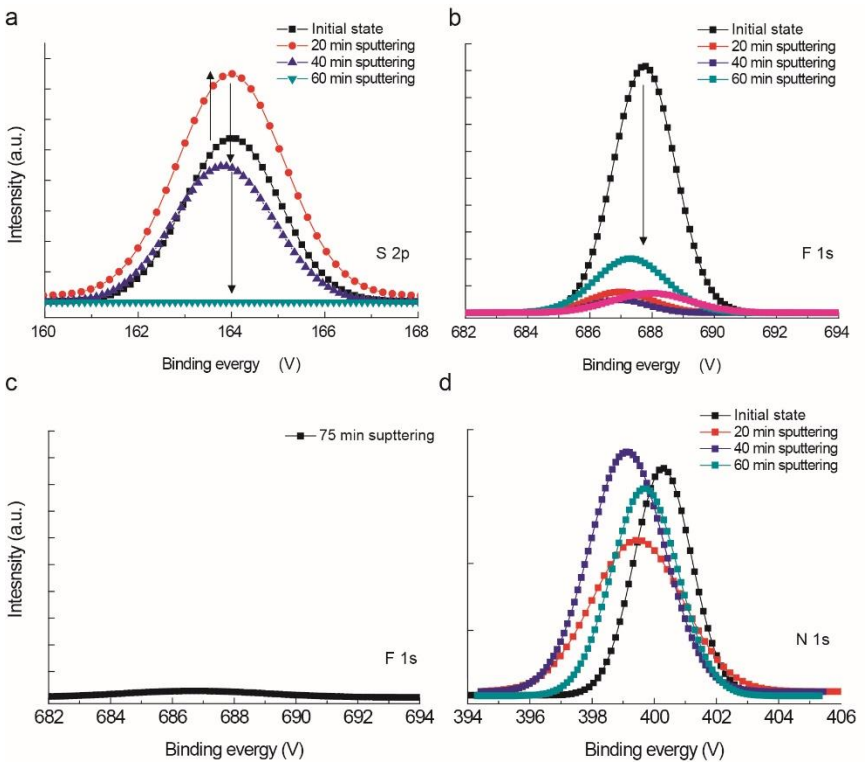

Figure S2. XPS depth profiling of P3HT/SiO_2 exposed to 1 mg/ml F4TCNQ. XPS spectra of the doped P3HT film depending on sputtering times: (a) sulfur, (b) fluorine, (c) fluorine (longer time, 75 min) and (d) nitrogen. Overlaying F4TCNQ on the P3HT surface indicated solubility limit of F4TCNQ in P3HT and would result in the saturated $V_{th,RG}$ shift in our RG FET under high concentration of F4TCNQ solutions. After continuing sputtering this film, sulfur peak steadily reduced and eventually disappeared because of completely removed P3HT from the SiO_2 surface. Accordingly, higher intense peak of fluorine was observed at the initial state (Figure S2b). Fluorine peaks from the sputtered P3HT films showed that a similar amount of the reduced dopants existed from the shallow surface through SiO_2 surface. Remaining F4TCNQ on SiO_2 surface even after 60 min sputtering (Figure S2b) was totally removed for further sputtering (75 min) as shown in Figure S2c. Not clear propensity was shown in nitrogen spectrum (Figure S2c). However, it clearly showed that F4TCNQ existed crossover the film. Changing in binding

energy in the nitrogen spectrum could be interpreted as the change in electrostatic shielding effects and resultant changed binding energy of a core electron during long-term sputtering. In addition, surface charging results in a change in the sample conductivity which can be altered by the incorporation of argon sputtering treatment.

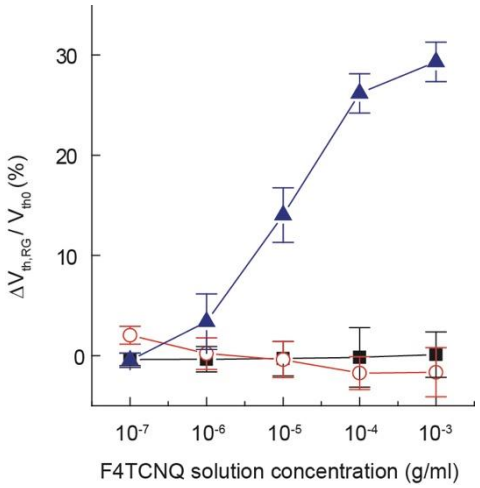

Figure S3. Distributions of normalized $V_{th,RG}$ variation of Figure 2c with respect to initial V_{th} (V_{th0}) from each RG. $\Delta V_{th,RG}$ was calculated by subtracting $V_{th,RG}$ values at each F4TCNQ solution concentration from V_{th0}.

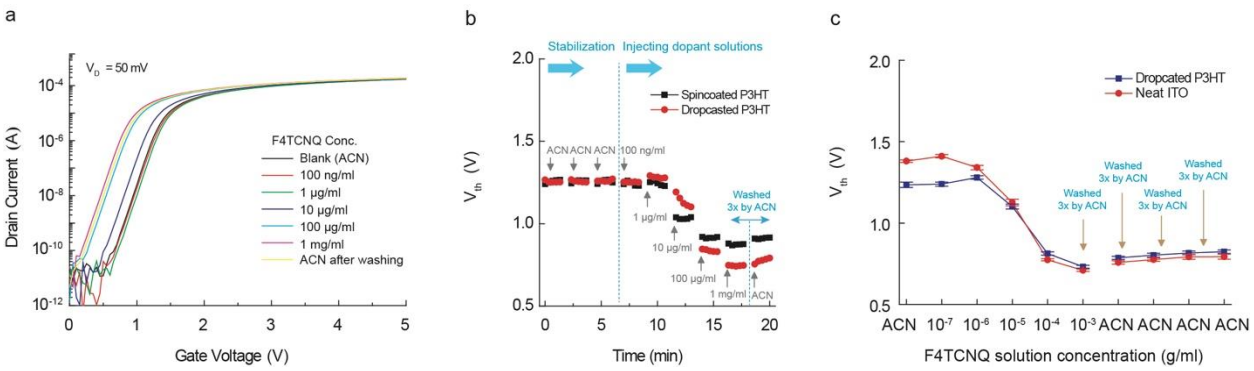

Figure S4. (a) Representative transfer curves of RG FET with dropcasted P3HT on the RG. (b) Time vs $V_{th,RG}$ values of FET from the RGs with spincoated and dropcasted P3HT. More $V_{th,RG}$ shifts were observed for the dropcasted P3HT RG over our testing F4TCNQ solution concentrations. (c) F4TCNQ solution concentrations vs $V_{th,RG}$ from the RG with the neat ITO and dropcasted P3HT.

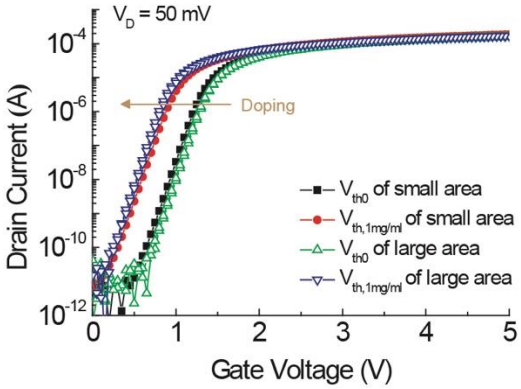

Figure S5. Response of transfer curve of RG FET from P3HT/SiO_2 RG with large and small doping area for F4TCNQ solutions (0.5 cm diameter vs 2 cm diameter). V_{th0} and $V_{th,RG}$ at 1 mg/ml F4TCNQ ($V_{th,1mg/ml}$) from different doping areas were in a similar level.

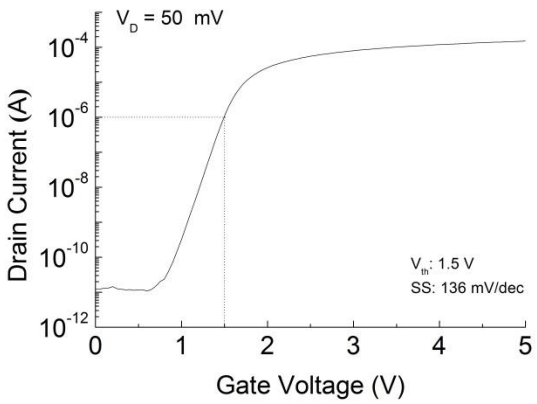

Figure S6. Transfer curve of intrinsic silicon FET. $V_{th,FET}$ was calculated by the gate voltage that corresponds to drain current of 1 μA and was measured to be 1.5 V.

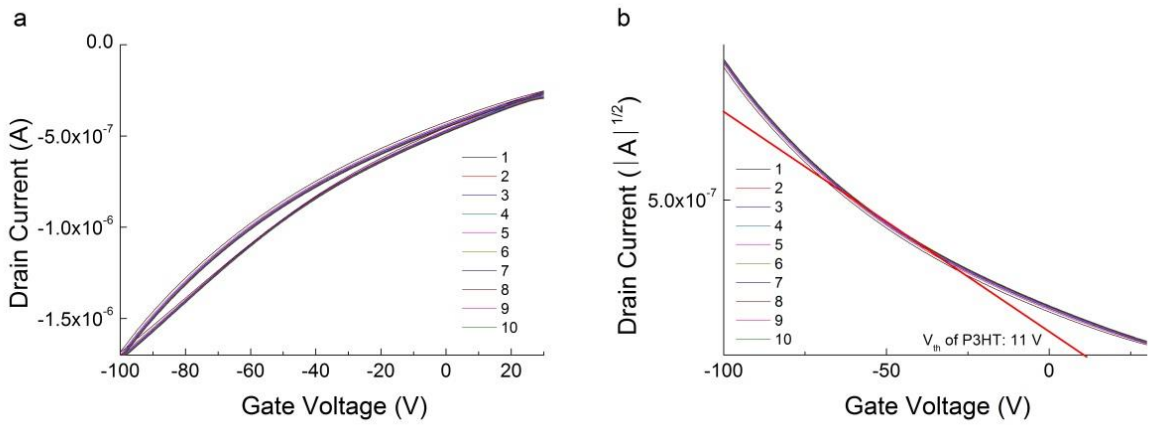

Figure S7. (a) Transfer curve of P3HT OFET. Transfer curves were repeated for 10 times under the double sweeping mode. Drain voltage was set as -100 V. A 300-nm-thick SiO_2 dielectric was used as gate dielectric. Width and length of OFET was 2 mm and 0.25 mm, respectively. (b) $\sqrt{|I_D|}$ vs gate voltage plot. V_{th} of P3HT OFET calculated from this plot was measured to be 11 V. Hole mobility at saturation regime was calculated to be 0.008 cm^2/Vs at V_g of -40 V by using following equation:

$$I_D = \frac{W}{2L}\mu_{sat}C_i\left(V_g - V_{th}\right)^2$$

where I_D is drain current and C_i is capacitance per area of gate dielectric.

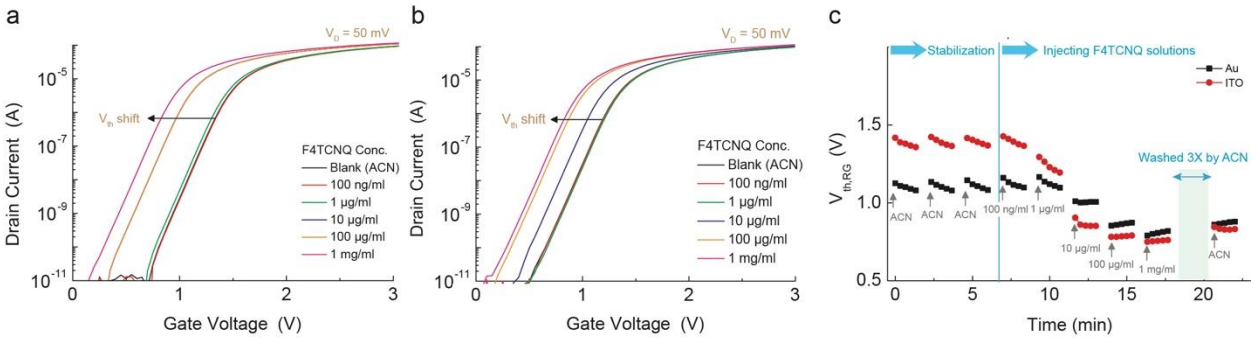

Figure S8. Response of transfer curves of RG FET with (a) ITO and (b) Au RGs for different F4TCNQ solution concentrations. (c) Representative $V_{th,RG}$ response from RGs of ITO and Au over time for F4TCNQ solution concentrations.

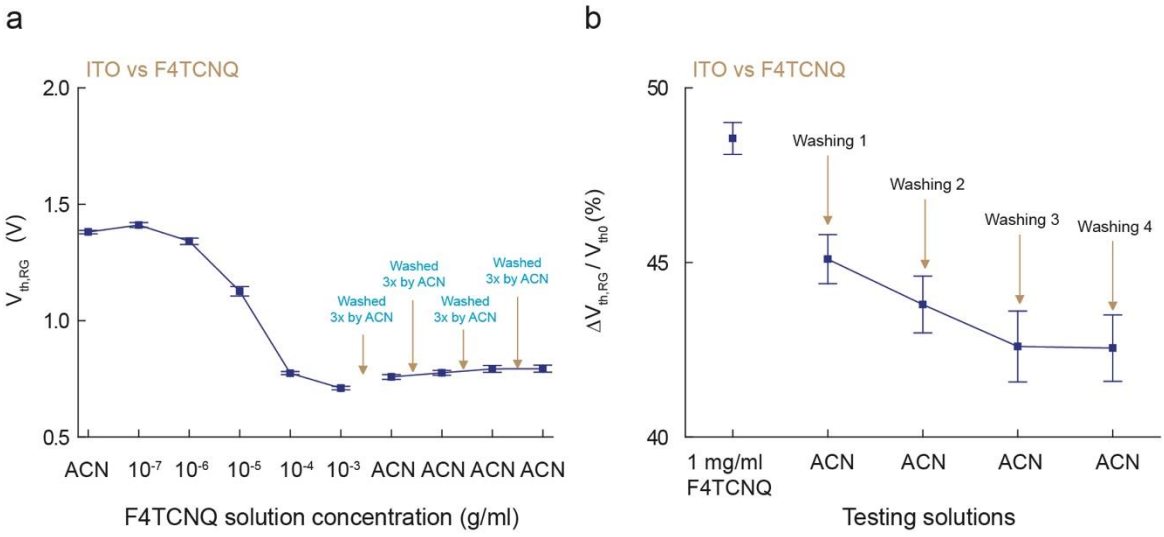

Figure S9. (a) $V_{th,RG}$ vs F4TCNQ solution concentrations with 4 more washing steps. (b) Variation of $V_{th,RG}$ at 1 mg/ml F4TCNQ and the neat ACN after each washing step with respect to V_{th0}.

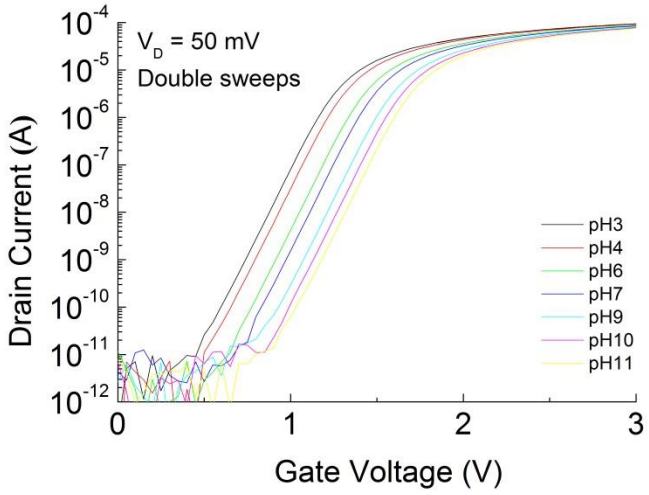

Figure S10. Representative transfer curve shift by ITO RG contacted to each pH buffer solution.

Equation details (Figure S11)

We calculated hole concentrations of the doped P3HT (p_d) using spectra of UV-Vis NIR spectra with the following equation:

$$c = \frac{A}{\varepsilon l}$$

where c is molar charge carrier concentration, l is thickness of the P3HT film (46 nm), A is absorbance of the species formed after doping, and ε is molar extinction coefficient. A value was calculated by subtracting absorption peak at 644 nm (baseline) from that of F4TCNQ at 771 nm was obtained. ε of $2 \times 10^5\ /Mcm$ was used according to the literature value for P3HT (Journal of Colloid and Interface Science 2017, 488 373–389). Finally, the accutal p_d in the doped P3HT was obtained from the following equation:

$$p_d = c \times 6.023 * 10^{23}$$

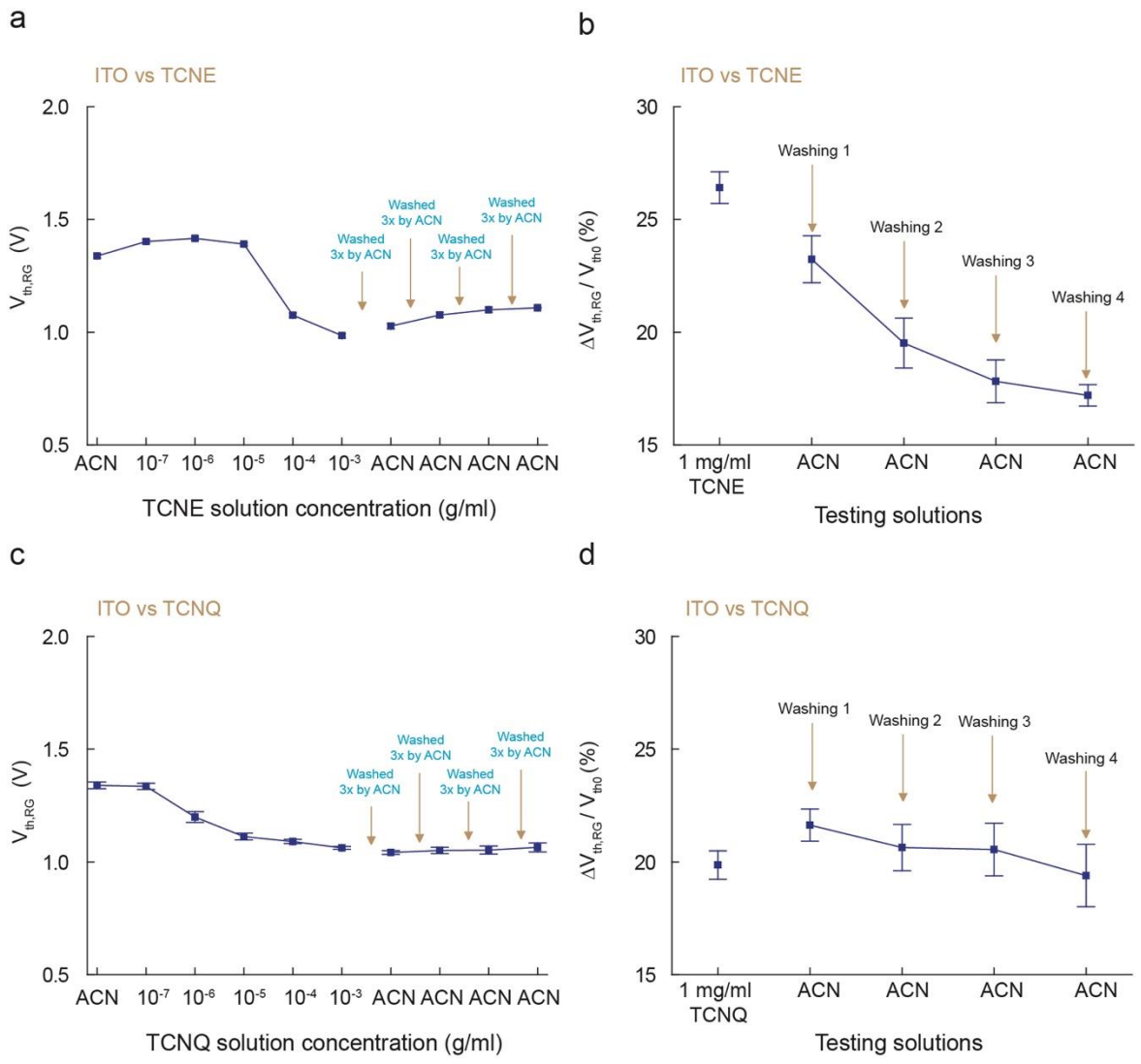

Figure S12. (a) $V_{th,RG}$ vs TCNE solution concentrations with 4 washing steps. (b) $V_{th,1mg/ml}$ variation of TCNE in terms of V_{th0} after washing. (c) $V_{th,RG}$ vs TCNQ solution concentrations with 4 washing steps. (d) $V_{th,1mg/ml}$ variation of TCNQ in terms of V_{th0} after washing.

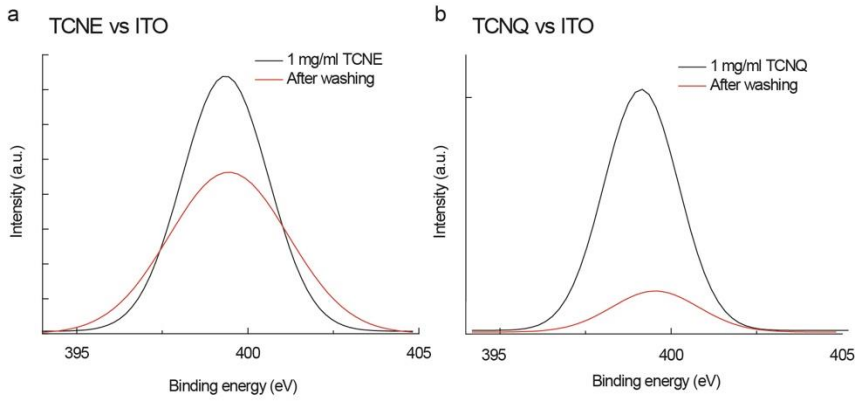

Figure S13. XPS spectra regarding N 1s peak from (a) TCNE:ITO and (b) TCNQ:ITO surfaces before/after washing. ITO surfaces doped by each dopant solution concentration of 1 mg/ml were washed by the neat ACN for 5 sec.

Table S1. Electrical parameters used in Figure 3g: conductivity, $\Delta V_{th,RG}$, hole concentrations of doped P3HT calculated by $V_{th,RG}$ shifting model of RG FET and UV-Vis-NIR spectra. $\Delta V_{th,RG}$ was calculated by using average values of each $V_{th,RG}$. Mobility was calculated based on hole concentrations by $V_{th,RG}$ shifting model and $\sigma = e\mu_h p_0$. Initial hole concentration was calculated to be 2.37×10^{-17} cm^{-3} based on μ_H from OFET (Figure S7) and conductivity (σ) using $\sigma = e\mu_h p_0$.

Samples	σ (S/cm)	$\Delta V_{th,RG}$ (V)	p (cm^{-3}) : RG	p (cm^{-3}) : UV-Vis NIR	μ_H (cm^2/Vs) : RG
Neat P3HT	3.18E-4	1.24 (initial)	2.37×10^{-17} (initial)	N/A	8.39×10^{-3}
100 ng/ml F4TCNQ : P3HT	3.57E-4	0.0059	1.88×10^{17}	N/A	1.18×10^{-2}
1 µg/ml F4TCNQ : P3HT	2.91E-4	-0.041	1.17×10^{18}	N/A	1.55×10^{-3}
10 µg/ml F4TCNQ : P3HT	0.081	-0.174	2.01×10^{20}	9.36×10^{21}	2.52×10^{-3}
100 µg/ml F4TCNQ : P3HT	0.933	-0.327	7.47×10^{22}	9.23×10^{22}	7.80×10^{-5}
1 mg/ml F4TCNQ : P3HT	9.88	-0.367	3.42×10^{23}	1.75×10^{23}	1.80×10^{-4}
After washing	Not measured	-0.309	3.72×10^{22}	Not measured	Not measured